EFFECT OF MULTI-WALLED CARBON NANOTUBES ON POLY(BUTYL METHACRYLATE-CO-ACRYLIC ACID)/POLY(N-VINYL-2-PYRROLIDONE) NANOCOMPOSITES

Guoqin LIU[1]*, Mengyao HOU[2], Fang HUANG[3]

Butyl methacrylate (BMA) and acrylic acid (AA) were copolymerized and crosslinked in the presence of acid-treated multi-walled carbon nanotubes (a-MWCNTs) and poly(N-vinyl-2-pyrrolidone) (PNVP) to obtain P(BMA-co-AA)/PNVP/MWCNTs nanocomposites. The morphology and mechanical properties of the nanocomposites were studied. Scanning electron microscopy (SEM) and transmission electron microscopic (TEM) analysis revealed a uniform distribution of MWCNTs in polymer matrix. The Young's modulus of the nanocomposites increased and the elongation at break decreased with increasing MWCNTs contents from 0.5 to 3.0 wt%. The Izod impact strength and tensile strength of materials, however, exhibited notable drop at MWCNTs concentration higher than 2.0 wt.%.

Keywords: nanocomposites, poly(butyl methacrylate-co-acrylic acid)/poly(N-vinyl-2-pyrrolidone), multi-walled carbon nanotubes .

1. Introduction

Although polymers have many advantages, such as lightweight, easy processing and resistance to chemical corrosion, their inherent disadvantages, poor thermal and mechanical properties, have limited their wide application. Therefore, it is a common method to modify polymers to expand their applications; among them, fabricating polymer-based nanocomposite is a frequently used modification method [1-4]. Nanoparticles can increase the strength of polymers, and the polymer-based nanocomposites are also manufactured by conventional processing methods, which make them more competitive from a cost perspective.

Carbon nanotubes (CNTs) are wide-ranging applications for the fabrication of polymer-based nanocomposites, because of their excellent combination of mechanical strength, thermal and electrical conductivity, and low mass density [5-9]. Two kinds of CNTs are usually used in a variety of

[1] Prof., College of Material Science and Engineering, Henan University of Technology,China.
*Corresponding Author: polymerpaper@163.com
[2] MS Sci., College of Material Science and Engineering, Henan University of Technology, China.
[3] Assoc. Prof., Eng., Henan University of Technology, China.

nanocomposites, *i.e.*, single-walled carbon nanotubes (SWCNTs) and MWCNTs [10]. Due to their easy dispersion and low cost, MWCNTs are more widely used to prepare polymer-based nanocomposites than SWCNTs [11, 12].

Generally, AA and BMA are selected as comonomers to prepare copolymers for adhesives and coatings; being parts of copolymers, their polymers provide adhesion and flexibility, respectively. PNVP can be used as not only a dispersant and stabilizer for nanoparticles, but also a carrier in drug delivery [13-15]. In recent years, poly (acrylic acid) (PAA) and poly(butyl methacrylate) (PBMA) are also applied for biomedicines [16-18].

In this study, P(BMA-co-AA)/PNVP/MWCNTs nanocomposites are synthesized and can be used as potential biomaterials. The influences of various MWCNTs loading on the morphology, Izod impact strength, tensile strength, Young's modulus, elongation at break, thermal properties, and swelling characteristics of P(BMA-co-AA)/PNVP/MWCNTs nanocomposites are studied and the nanocomposites are expected to use widely in medicine.

2. Experimental

2.1. Materials

MWCNTs were bought from Shenzhen Nanotech Port. BMA, AA, and 2,2'-azobis(isobutyronitrile) (AIBN) were purchased from Chengdu Reagent Factory (China). In order to remove the polymerization inhibitors, BMA and AA were purified separately by decompressing distillation. AIBN was refined by recrystallization in ethanol solution and acted as an initiator. N,N'-methylenebis(acrylamide) (MBAA, Aldrich) as a cross-linker, and PNVP (Aldrich, M_n = 30000) as an organic dispersant, were used without further treatment.

2.2. Preparation of P(BMA-co-AA)/PNVP/MWCNTs nanocomposites

2 g MWCNTs were soaked in 60 ml H_2SO_4/HNO_3 (3:1 v/v) and refluxed for 6 hours. Then, the acid-treated MWCNTs (a-MWCNTs) were rinsed in distilled water till the pH of the flushing fluid was close to 7. Finally, the filtered a-MWCNTs were dried in a vacuum oven for use. The concentrations of BMA and AA remained 1:1 (mol/mol) with changes in a-MWCNTs content. Firstly, a-MWCNTs were immersed in 50 ml dimethyl sulfoxide (DMSO), and then ultrasonicated for 1 hours; the amount of a-MWCNTs addition was 0.5, 1.0, 2.0 and 3.0 wt% (relatively to total weight of BMA and AA, TW), respectively; subsequently, BMA (1.5 mol·L^{-1}), AA (1.5 mol·L^{-1}), PNVP (25 wt% of TW), AIBN (0.02 mol·L^{-1}), and MBAA (0.1 mol·L^{-1}) were put into a-MWCNTs. The mixtures were ultrasonicated for 1 hours; then, N_2 was fed into the mixture to remove O_2; the mixture was rapidly heated to 65 °C, uniformly stirred and sonicated for 0.5 hour, soon afterwards cooled to 55 °C, injected into a flat glass

mold, and proceeded to polymerize for 24 hours, as depicted in Fig. 1; the products obtained, *i.e.*, P(BMA-co-AA)/PNVP/MWCNTs nanocomposites, were dried under vacuum at 70 °C for 72 hours in order to get rid of unreacted monomers and DMSO.

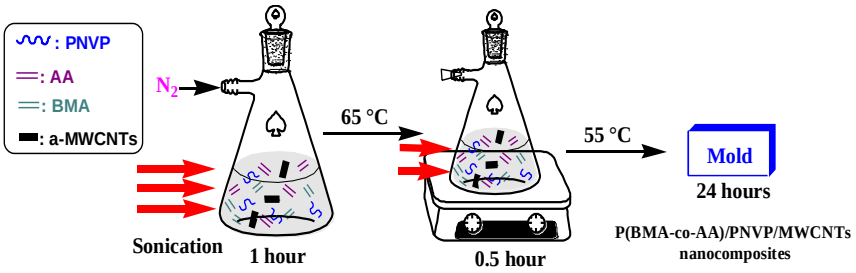

Fig. 1. A schematic diagram of preparation ofP(BMA-co-AA)/PNVP/MWCNTs nanocomposites.

2.3. Characterization

Raman spectra (Renishaw 1000 NR) were acquired under room conditions with a 633 nm excitation laser. Fourier transform infrared spectroscopy (FTIR 8300PCS, Shimadzu) was used to characterize the specific functional groups at a resolution of 2 cm^{-1}; the dried powder sample were examined as pressed KBr disks. The cryo-sections of 100 nm thickness were gotten by Leica EM UC6 and studied with TEM (FEI Fecnai G^2 F_{20} S-Twin). The fractured surface was obtained in liquid N_2, sputtered gold coating and observed with SEM (JSM-5900LV). SEM and TEM were operated at an accelerating voltage of 20 and 200 kV, respectively. The notched Izod impact strength was tested using acute notched specimens (tested samples with sizes of 80 mm×10 mm×4 mm, notch depth: 2 mm) at 23 ˚C with XJ-40A pendulum apparatus (China). In order to calculate the mean values and standard deviation of the experiments results, five samples were parallelly tested following ASTM D-256 method. A universal tensile machine (Instron, model 4302) was chosen to measure tensile properties of the dog bone-shaped specimens (60 mm×10 mm×4 mm) at crosshead rate of 5 $mm \cdot min^{-1}$. The decomposition temperature was measured by thermogravimetric analysis (TGA, Perkin-Elmer) under air from room temperature to 665 ˚C at a heating rate of 10 $^{\circ}C \cdot min^{-1}$.

Swelling property was characterized by weighing absorbing water content. First, about 2 g of the rectangular-shaped sample with approximately 20 mm length, 5 mm width and 2 mm thickness was dried to constant weight under vacuum; subsequently, it was taken out and immersed in 1000 ml deionized water at 27 °C for 72 hours (The sample was considered to reach swelling equilibrium); the swelling sample was taken out; its surface water was wiped off with absorbent

paper, and then weighed. In swelling equilibrium state, the swelling degree (D_s) and the water content (C_w) were calculated separately from the following relation:

$$D_s = (W_{sw} - W_{dw}) / W_{dw} \times 100 \quad (1)$$

$$C_w = (W_{sw} - W_{dw}) / W_{sw} \times 100 \quad (2)$$

Where W_{sw} and W_{dw} are the swollen weight at equilibrium state and the vacuum-dried constant weight of the tested sample, respectively.

3. Results and Discussion

There is no doubt that the uniform dispersion of CNTs is important for making full use of their characteristics. After mixed acids treatments, as result of forming oxidation fragments on MWCNTs surface, *i.e.*, carboxylated carbonaceous debris, the structural defects on their surfaces increase [19]. Raman spectroscopy can be made use of researching their defects. Fig. 2 shows Raman spectra of pristine MWCNTs and a-MWCNTs; their shapes are the same, indicating that the mixed acid treatment don't destroy the graphite structure of MWCNTs. D-band and G-band present at around 1351 and 1580 cm^{-1}, respectively; D-band results from a double resonance scattering owing to structural defects existence, and yet G-band is caused by the tangential in-plane vibration of graphitic C atoms. Ratio of D *vs* G band intensities (I_D/I_G ratio) can reflect defect quantity in MWCNTs, the higher the I_D/I_G ratio, the greater the amount of structural defects. The I_D/I_G ratio of prinstine MWCNTs and a-MWCNTs is 0.38 and 0.76, respectively. By comparing their I_D/I_G ratios, it can be concluded that mixed acid treatment introduces more defects to MWCNTs structure, namely carboxylated carbonaceous debris. Those mean the carboxylic acid functionalized MWCNTs form and are conducive to their dispersion.

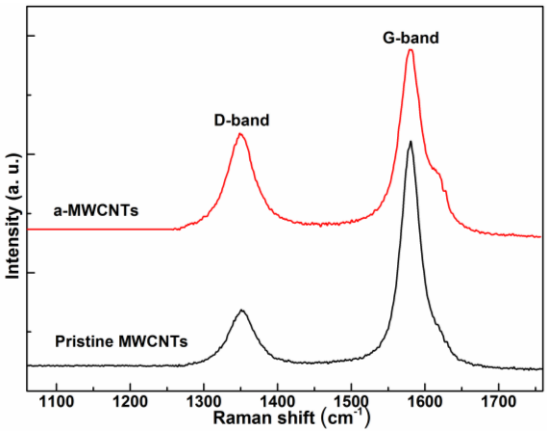

Fig. 2. Raman spectra of prinstine MWCNTs and a-MWCNTs.

Treated by mixed acids, the surfaces of MWCNTs are oxidized and form

some functional groups, for example, carboxylic acid groups (-COOH) [21, 21], which undoubtedly increase the interfacial force between the polymer and the MWCNTs and thus facilitates their dispersion. Fig. 3 is FTIR spectrum of MWCNTs, a-MWCNTs, P(BMA-co-AA)/PNVP and P(BMA-co-AA)/PNVP/3.0 wt% MWCNTs.

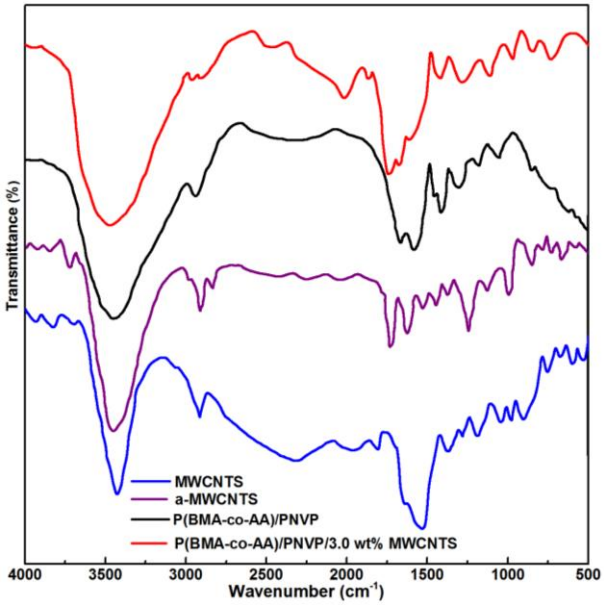

Fig. 3. FTIR spectrum of MWCNTs, a-MWCNTs, P(BMA-co-AA)/PNVP and P(BMA-co-AA)/PNVP/MWCNTs.

The peak at 2913 cm^{-1} corresponds to C-H of the a-MWCNTs and MWCNTs. The peak at 1528 cm^{-1} comes from the hexagonal structure of CNTs, meaning the existence of C=C. In terms of a-MWCNTs, due to oxidation of carbon, the new peak at 1726 cm^{-1} emerges, which attributes to C=O stretching vibration of carboxyl groups [22, 23]. The C=C at 1528 cm^{-1} and the hexagonal carbon between 500 and 1000 cm^{-1} are attacked by mixed acid, which reduces the peak intensity. Decreasing of the peak intensity derives from the existence of a lot of asymetrical hexagonal carbon. At 1625 cm^{-1}, the peak intensity of a-MWCNTs is much weaker than that of MWCNTs, due to decreasing carbonyl of quinone type units on the surface of MWCNTs after acid treatments. The above analysis shows there are -COOH groups on the sidewalls of MWCNTs. For P(BMA-co-AA)/PNVP, because of the superposition of the stretching vibration absorption peak of C=O in PNVP and the asymmetric stretching vibration peak of C-O in AA, there is a broad infrared absorption peak at 1668 cm^{-1}. After the introduction of MWCNTs in P(BMA-co-AA)/PNVP, in comparison to P(BMA-co-AA)/PNVP and a-MWCNTs, a wide peak around 3478 cm^{-1} corresponding to OH vibration appears; meanwhile, C=O stretching vibration of the nanocomposites shifts to a

longer wavenumber of 1744 cm^{-1}, which is due to the groups interaction between P(BMA-co-AA)/PNVP and MWCNTs or the formation of hydrogen bonds.

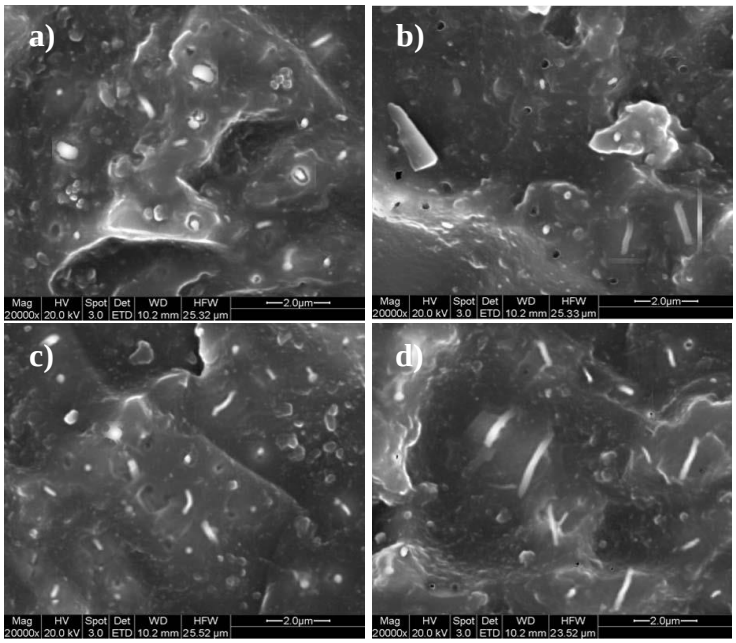

Fig. 4. SEM images of P(BMA-co-AA)/PNVP/MWCNTs nanocomposites. a) 0.5 wt% MWCNTs; b) 1.0 wt% MWCNTs; c) 2.0 wt% MWCNTs; d) 3.0 wt% MWCNTs.

The SEM images of P(BMA-co-AA)/PNVP/MWCNTs nanocomposites' cryo-fractured surface are illustrated in Fig. 4. Due to the nanocomposites elongation at break, the fibrous fractured morphology can be observed. One end of some MWCNTs is firmly inserted into the polymer matrix and the other end is pulled and exposed out of the nanocomposites, which means there is a strong interfacial adhesion between MWCNTs and P(BMA-co-AA)/PNVP. The enhancement of CNTs depends not only on its own strength but also on the interfacial strength between CNTs and polymer. By the strong interfaces force resulting from the interaction of their functional groups, the load can effectively transfer from the polymer to MWCNTs, and then pass to the polymer matrix again. As result of MWCNTs high conductivity [24], the ends of MWCNTs display as some dispersed bright dots in the electric field of SEM. On the other hand, there are some caves on the fractured surface in Fig. 4, which is attributed to some MWCNTs pulled out of the polymer matrix because the tensile force is large enough to overcome the interfacial adhesion between MWCNTs and P(BMA-co-AA)/PNVP. In Fig. 4, no matter the bright dots (i. e., the ends of MWCNTs) or the caves (as a result of MWCNTs pulling out from P(BMA-co-AA)/PNVP), they can both uniformly disperse, indicating MWCNTs are evenly distributed in the polymer likely because of their functional groups' interaction. With increasing of

MWCNTs content, after acid treating, the interaction between MWCNTs and P(BMA-co-AA)/PNVP promotes the dispersion of MWCNTs in the polymer matrix.

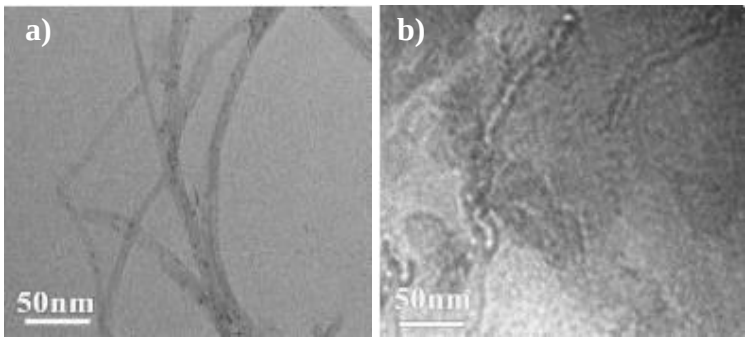

Fig. 5. TEM images of a-MWCNTs (**a)**) and P(BMA-co-AA)/PNVP/3.0 wt% MWCNTs nanocomposites (**b)**).

To gain a deeper insight into MWCNTS distribution, TEM analysis was observed their dispersion. Fig. 5 represents the TEM images of a-MWCNTs and P(BMA-co-AA)/PNVP/3.0 wt% MWCNTs nanocomposites. Compared with Fig. 5 a), it can be clearly observed that MWCNTs are uniformly distributed in the polymer matrix in Fig. 5 b), which is basically consistent with the previous observations of SEM. Moreover, the interface between the matrix and becomes wider and vague, which can arise from their interaction, i.e., hydrogen bonds mentioned above.

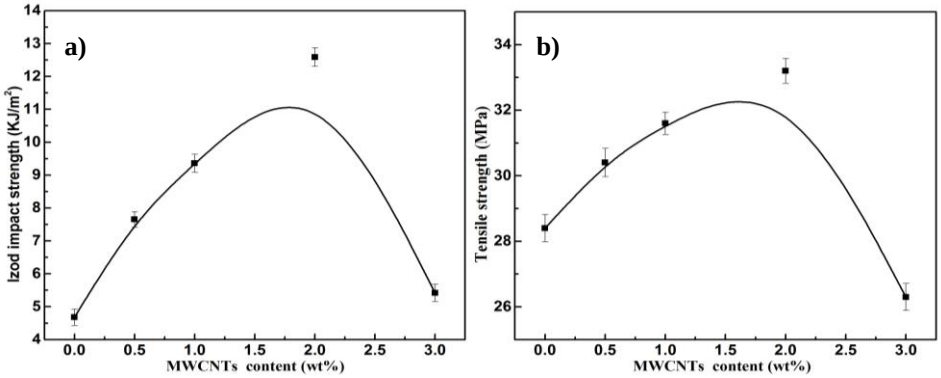

Fig. 6. Izod impact strength (**a)**) and Tensile strength (**b)**) of P(BMA-co-AA)/PNVP and its nanocomposites.

The main goal of designing nanocomposites is to improve the mechanical properties of materials. The addition of MWCNTs is bound to affect the impact strength of P(BMA-co-AA)/PNVP/MWCNTs nanocomposites; the variation of notched Izod impact strength with MWCNTs' contents is shown in Fig. 6 a). When the content of MWCNTs increases, their distribution is uniform, as shown

in Fig. 4, and the Izod impact strength enhances with increasing of MWCNTs contents and achieves 12.59 J/m^2 at 2.0 wt% MWCNTs; compared with that of P(BMA-co-AA)/PNVP, the impact strength of P(BMA-co-AA)/PNVP/MWCNTs nanocomposites is a 169% increasing, which proves from the side that the uniform dispersion of the MWCNTs is advantageous in improving the impact strength. The a-MWCNTs is likely to forming hydrogen bonds with P(BMA-co-AA)/PNVP; when the nanocomposites are subjected to an impact force, the hydrogen bonds between MWCNTs and P(BMA-co-AA)/PNVP is broken; which makes the nanocomposites bear more external load. As a result, the impact strength gradually increases as the content of MWCNTs increased. With the further increase of MWCNTs contents (> 2 wt%), the impact strength shows a decreasing trend. Higher contents of MWCNTs easily give rise to stress concentration, which reduces the impact strength of the nanocomposite.

CNTs have an enhanced effect on the polymer mechanical properties. The tensile strength of P(BMA-co-AA)/PNVP/MWCNTs nanocomposites with different contents MWCNTs was measured, as shown in Fig. 6 b). Due to the introduction of MWCNTs, the variation trend of the nanocomposites' tensile strength is similar with that of their impact strength; in comparison to P(BMA-co-AA)/PNVP, the tensile strength of the nanocomposite is initially increased until the MWCNTs content is 2.0 wt%, increasing 17%, and subsequently reduces with increasing of MWCNTs content. The reason may be related to the contents of MWCNTs; The appropriate amount of MWCNTs effectively plays the role of their reinforcing agent. Conversely, an excessively high MWCNTs content easily cause stress concentration.

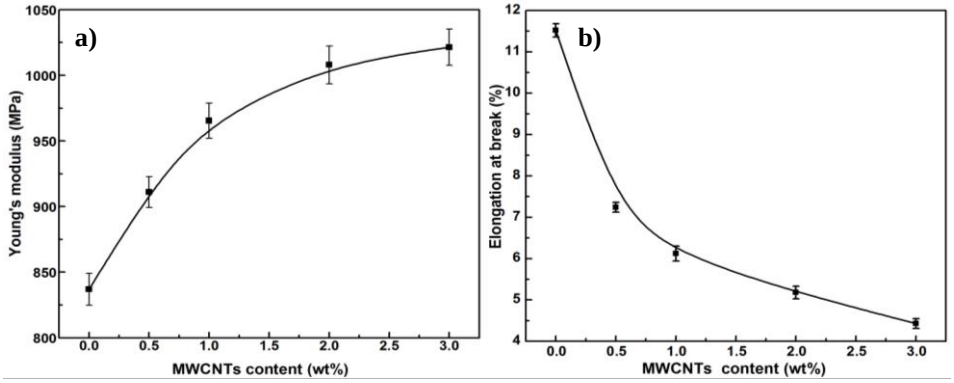

Fig. 7. Young's modulus (**a)**) and Elongation at break (**b)**) of P(BMA-co-AA)/PNVP and its nanocomposites.

Fig. 7 a) shows the Young's modulus of P(BMA-co-AA)/PNVP/MWCNTs nanocomposites with different MWCNTs contents. The modulus of the nanocomposites increases with increasing of MWCNTs content and is about 1021 MPa when the content of MWCNTs is 3 wt%, increasing 22% in comparison with

that of P(BMA-co-AA)/PNVP. These results indicate that an increase in the MWCNTs content of the nanocomposites leads to increasing stiffness. It is clear that a higher content of MWCNTs will result in a transition of materials from toughness to brittleness. Fig. 7 b) shows the elongation at break of the nanocomposites with different MWCNTs contents. As analyzed above, the addition of MWCNTs significantly increases P(BMA-co-AA)/PNVP rigidity. In Fig. 7 b), a obvious decrease of the elongation at break can be observed as the MWCNTs content increase. Compared with P (BMA-co-AA)/PNVP, the maximum elongation at break of nanocomposites decreases up to 62%. It is clear that MWCNTs are very rigid and almost no elongation. When MWCNTs are blended with the polymer, they are bound to increase the rigidity of the polymer and restrict polymer segments' movement. Consequently, MWCNTs restrain the materials elongation, making them less ductile.

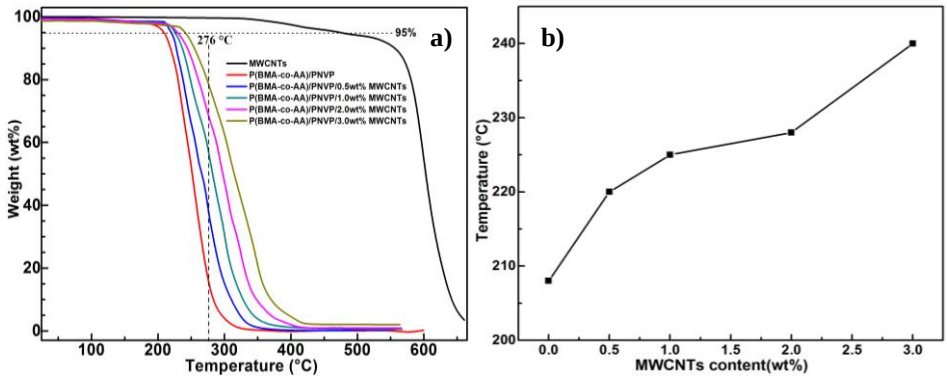

Fig. 8.TGA of MWCNTs, P(BMA-co-AA)/PNVP and P(BMA-co-AA)/PNVP/MWCNTs (**a)**) and T_d *vs* MWCNTs contents (**b)**) .

Generally, the introduction of CNTs into the polymer can improve the heat resistance of the polymer. The TGA thermograms of MWCNTs, P(BMA-co-AA)/PNVP and its nanocomposites are shown in Fig. 8 a). MWCNTs have a high thermal stability and their weight loss is less than 5 wt% at temperatures below 473 ˚C. The degradation temperature (onset of inflection) of P(BMA-co-AA)/PNVP/MWCNTs nanocomposites is higher than that of P(BMA-co-AA)/PNVP, and is increased by at least 12 ˚C. The weight loss of P(BMA-co-AA)/PNVP/MWCNTs nanocomposites are between 38 % and 78% at 276˚C; the more the MWCNTs content of the nanocomposites is, the less the weight loss is; but the weight loss P(BMA-co-AA)/PNVP is up to 85%. These results demonstrate MWCNTs can improve the thermal stability of P(BMA-co-AA)/PNVP.

In order to further figure out the relationship between the content of MWCNTs and the decomposition temperature (T_d, 5 wt % loss' temperature), the degradation temperature versus MWCNTs contents is shown in Fig. 8 b). T_d of the

P(BMA-co-AA)/PNVP and the MWCNTs are 209 and 473 ˚C, respectively. Once P(BMA-co-AA)/PNVP is introduced into MWCNTs, T_d of P(BMA-co-AA)/PNVP/MWCNTs nanocomposites significantly improves; T_d of the nanocomposites with 0.5 wt% MWCNTs has increased by more than 12 ˚C, that of the nanocomposites with 3 wt% MWCNTs by more than 32 ˚C. It can be seen from the above results that the contents of MWCNTs, even if they are very low, have an obvious influence on improving the heat resistance of polymer; the reason may be that the CNTs themselves have good heat resistance, and can improve the thermal conductivity of the nanocomposites when they are thermally degraded. However, the higher CNTs contents are not conducive to their dispersion, and may even form their aggregates, which in turn weaken the use of CNTs as reinforcing agents. It should be emphasized that the addition of CNTs can only finitely increase the thermal stability of the polymer.

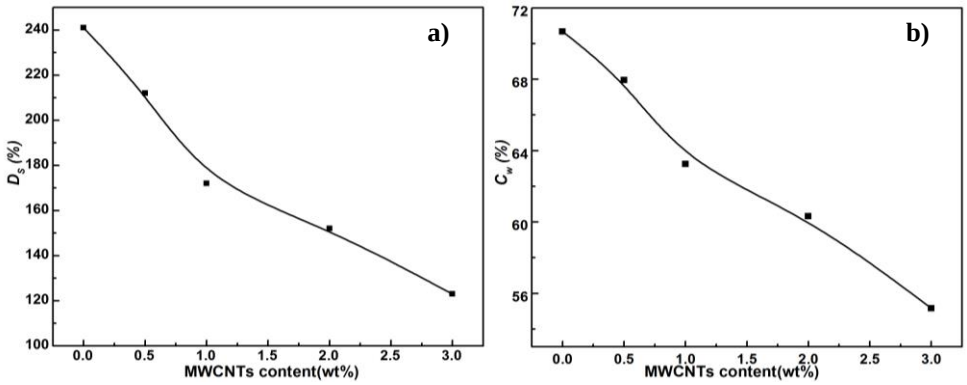

Fig. 9. D_s (**a)**) and C_w (**b)**) of P(BMA-co-AA)/PNVP/MWCNTs versus MWCNTs contents.

Because P(BMA-co-AA)/PNVP/MWCNTs nanocomposites have cross-linking structures and a certain of bio-compatibility, they might be acted as potential bio-materials. The degree of swelling is one of the important properties of gel. Fig. 9 a) and b) are D_s and C_w of P(BMA-co-AA)/PNVP/MWCNTs with different MWCNTs contents, respectively. The D_s and C_w of P(BMA-co-AA)/PNVP is more than those of the nanocomposites, which means that P(BMA-co-AA)/PNVP have a high water retention; as a result of the introduction of MWCNTs, with increasing of their contents, both D_s and C_w of the nanocomposites show a decreasing trend. Due to the functional groups interaction between MWCNTs and P(BMA-co-AA)/PNVP, on the one hand, it promotes the dispersion of MWCNTs, and on the other hand, MWCNTs also play a role of physical cross-linking. The dispersion of MWCNTs in P(BMA-co-AA)/PNVP may restrict the movement of polymer segment and might decrease polymer free volume, thus reducing the swelling of P(BMA-co-AA)/PNVP/MWCNTs.

4. Conclusions

After mixed acid treatment, the surface of MWCNTs was oxidized and formed -COOH functional groups, which increased the interfacial force between MWCNTs and P(BMA-co-AA)/PNVP and contributed to MWCNTs dispersion in the polymer matrix. The Izod impact strength and tensile strength of the nanocomposites increase originally, 167% and 17% increasing at at 2.0 wt% MWCNTs, respectively, and exhibited notable drop at MWCNTs concentration higher than 2.0 wt.%. Young's modulus of the nanocomposites increases with increasing of MWCNTs content (up to 22%), while the elongation at break of nanocomposites decreased by 62%. Meanwhile, MWCNTs can effectively improve the thermal stability of polymer, T_d of the nanocomposites with 3 wt% MWCNTs by more than 32 ˚C and decrease their swelling degree.

Acknowledgments

Financial support from the Science and Technology Project of Henan Province (No. 172102210033).

R E F E R E N C E S

[1] *M. Alsharabasy, A. Pandit, P. Farràs*, Recent advances in the design and sensing applications of hemin/coordination polymer-based nanocomposites, Advanced Materials, **vol. 33**, 2021, 2003883.

[2] *Chaurasia, R. S. Mulik, A. Parashar*, Polymer-based nanocomposites for impact loading: A review, Mechanics of Advanced Materials and Structures, **vol. 29**, 2022, 2581-2606.

[3] *Salabat, F. Mirhoseini*, Polymer-based nanocomposites fabricated by microemulsion method, Polymer Composites, **vol. 43**, 2022, 1282-1294.

[4] *Oseli, A. Vesel, E. Zagar, L. S. Perse*, Mechanisms of single-walled carbon nanotube network formation and its configuration in polymer-based nanocomposites, Macromolecules, **vol. 54**, 2021, 3334-3346.

[5] *Y. Zare, K. Y. Rhee*, A simple model for electrical conductivity of polymer carbon nanotubes nanocomposites assuming the filler properties, interphase dimension, network level, interfacial tension and tunneling distance, Composites Science and Technology, **vol. 155**, 2018, 252-260.

[6] *J. M. Zhu, Y. Zare, K. Y. Rhee*, Analysis of the roles of interphase, waviness and agglomeration of CNT in the electrical conductivity and tensile modulus of polymer/CNT nanocomposites by theoretical approaches, Colloids and Surfaces A: Physicochemical and Engineering Aspects, **vol. 539**, 2018, 29-36.

[7] *J. Cha, G. H. Jun, J. K. Park, J. C. Kim, H. J. Ryu, S. H. Hong*, Improvement of modulus, strength and fracture toughness of CNT/Epoxy nanocomposites through the functionalization of carbon nanotubes, Composites, Part B, **vol. 129**, 2017, 169-179.

[8] *A. Shayesteh Zeraati, S. A. Mirkhani, U. Sundararaj*, Enhanced dielectric performance of polymer nanocomposites based on CNT/MnO_2 nanowire hybrid nanostructure, The Journal of Physical Chemistry C, **vol. 121**, 2017, 8327-8334.

[9] *M. Aghelinejad, S. N. Leung*, Fabrication of open-cell thermoelectric polymer nanocomposites by template-assisted multi-walled carbon nanotubes coating, Composites, Part B, **vol. 145**, 2018, 100-107.

[10] *H. Ali-Boucetta, A. Nunes, R. Sainz, M. A. Herrero, B. Tian, M. Prato, A. Bianco, K. Kostarelos*, Inside cover: asbestos-like pathogenicity of long carbon nanotubes alleviated by chemical functionalization, Angewandte Chemie International Edition, **vol. 52**, 2013, 2130-2130.

[11] *S. H. Kim, W. I. Lee, J. M. Park*, Assessment of dispersion in carbon nanotube reinforced composites using differential scanning calorimetry, Carbon, **vol. 47**, 2009, 2699-2703.

[12] *H. Meng, G. X. Sui, P. F. Fang, R. Yang*, Effects of acid-and diamine-modified MWNTs on the mechanical properties and crystallization behavior of polyamide 6, Polymer, **vol. 49**, 2008, 610-620.

[13] *F. Alimohammadi, M. P. Gashti, A. Mozaffari*, Polyvinylpyrrolidone/carbon nanotube/cotton functional nanocomposite: preparation and characterization of properties, Fibers and Polymers, **vol. 19**, 2018, 1940-1947.

[14] *L. Luss, P. P. Kulikov, S. B. Romme, C. L. Andersen, C. P. Pennisi, A. O. Docea, A. N. Kuskov, K. Velonia, Y. O. Mezhuev, M. I. Shtilman, A. M. Tsatsakis, L. Gurevich*, Nanosized carriers based on amphiphilic poly-N-vinyl-2-pyrrolidone for intranuclear drug delivery, Nanomedicine, **vol. 13**, 2018, 703-715.

[15] *F. R. Vernosfaderani, D. Semnani*, Manufacturing and optimization the nanofibres tissue of poly (N-vinyl-2-pyrrolidone)-poly (e-caprolactone) shell/poly (N-vinyl-2-pyrrolidone)-amphotericin b core for controlled drug release system, Fibers and Polymers, **vol. 19**, 2018, 620-626.

[16] *M. Xu, J. Zhu, F. Wang, Y. Xiong, Y. Wu, Q. Wang, J.Weng, Z. Zhang, W. Chen, S. Liu*, Improved in vitro and in vivo biocompatibility of graphene oxide through surface modification: poly (acrylic acid)-functionalization is superior to PEGylation, ACS nano, **vol. 10**, 2016, 3267-3281.

[17] *K. Awsiuk, Y. Stetsyshyn, J. Raczkowska, O. Lishchynskyi, P. Dąbczynski, A. Kostruba, H. Ohar, Y. Shymborska, S. Nastyshyn, A. Budkowski*, Temperature-controlled orientation of proteins on temperature-responsive grafted polymer brushes: poly (butyl methacrylate) vs poly (butyl acrylate): morphology, wetting, and protein adsorption, Biomacromolecules, **vol. 20**, 2019, 2185-2197.

[18] *T. Ito, N. Otani, K. Fujii, K. Mori, M. Eriguchi, Y. Koyama*, Bioadhesive and biodissolvable hydrogels consisting of water-swellable poly (acrylic acid)/poly (vinylpyrrolidone) complexes, Journal of Biomedical Materials Research Part B: Applied Biomaterials, **vol. 108**, 2020, 503-512.

[19] *Y. Li, H. Li, A. Petz, S. Kunsági-Máté*, Reducing structural defects and improving homogeneity of nitric acid treated multi-walled carbon nanotubes, Carbon, **vol. 93**, 2015, 515-522.

[20] *H. Hu, P. Bhowmik, B. Zhao, M. A. Hamon, M. E. Itkis, R. C. Haddon*, Determination of the acidic sites of purified single-walled carbon nanotubes by acid-base titration, Chemical Physics Letters, **vol. 345**, 2001, 25-28.

[21] *H. Hu, B. Zhao, M. E. Itkis, R. C. Haddon*, Nitric acid purification of single-walled carbon nanotubes, The Journal of Physical Chemistry B, **vol. 107**, 2003, 13838-13842.

[22] *S. Chen, W. Shen, G. Wu, D. Chen, M. Jiang*, A new approach to the functionalization of single-walled carbon nanotubes with both alkyl and carboxyl groups, Chemical Physics Letters, **vol. 402**, 2005, 312-317.

[23] *S. Y. Lee, S. J. Park*, Hydrogen adsorption of acid-treated multi-walled carbon nanotubes at low temperature, Bulletin of the Korean Chemical Society, **vol. 31**, 2010, 1596-1600.

[24] *D. Chen, M. Wang, W. D. Zhang, T. Liu*, Preparation and characterization of poly (vinylidene fluoride) nanocomposites containing multiwalled carbon nanotubes. Journal of applied polymer science, **vol. 113**, 2009, 644-650.